

Briefing Space Weather

2022/09/27

1 Sun

1.1 Responsible: José Cecatto

09/19 – No flare (M/X); Fast wind stream (≤ 550 km/s); 2 CME c.h.c. toward the Earth;
 09/20 – M1.1 flare; Fast wind stream (≤ 550 km/s); 7 CME c.h.c. toward the Earth;
 09/21 – M1.1 flare; Fast wind stream (≤ 550 km/s); 5 CME c.h.c. toward the Earth;
 09/22 – No flare (M/X); Fast wind stream (≤ 450 km/s); 6 CME c.h.c. toward the Earth;
 09/23 – M1.8 flare; Fast wind stream (≤ 500 km/s); 12 CME c.h.c. toward the Earth;
 09/24 – No flare (M/X); Fast wind stream (≤ 500 km/s); 8 CME c.h.c. toward the Earth;
 09/25 – No flare (M/X); No fast wind stream; 2 CME c.h.c. toward the Earth;
 09/26 – No flare (M/X); No fast wind stream; No CME c.h.c. toward the Earth;
 Prev.: Fast wind stream expected on September 26-27 and October 01; for the next 2 days (40% M, 10% X)
 probability of M / X flares; also, occasionally other CME can present component toward the Earth.
 c.h.c. – can have a component; * partial halo; ** halo

2 Sun

2.1 Responsible: Douglas Silva

- WSA-ENLIL (Prediction for CME : 2022-09-22T07:36Z)
 - The simulation results indicate that the flank of CME will reach the DSCOVR mission between 2022-09-26T01:00Z and 2022-09-26T15:00Z.

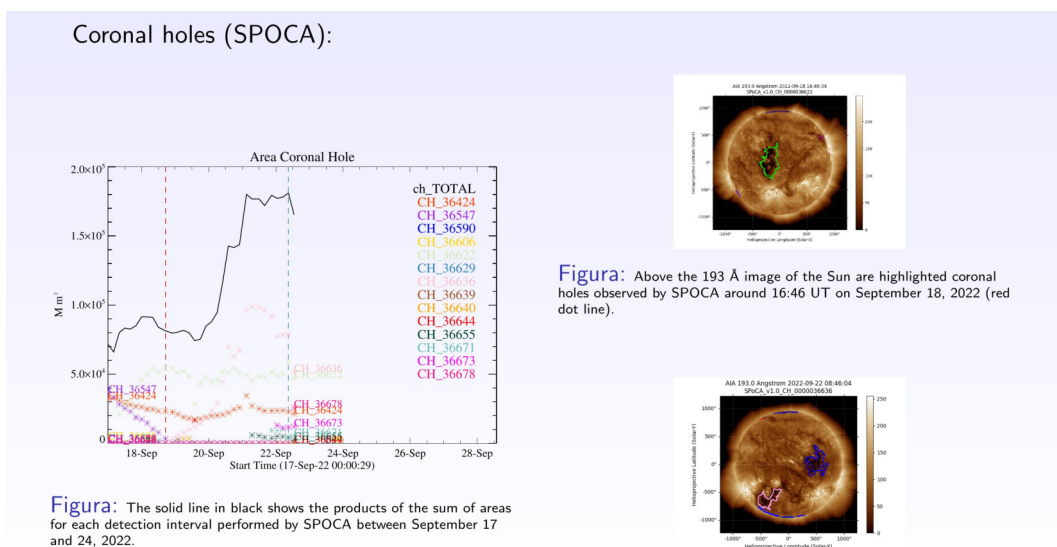
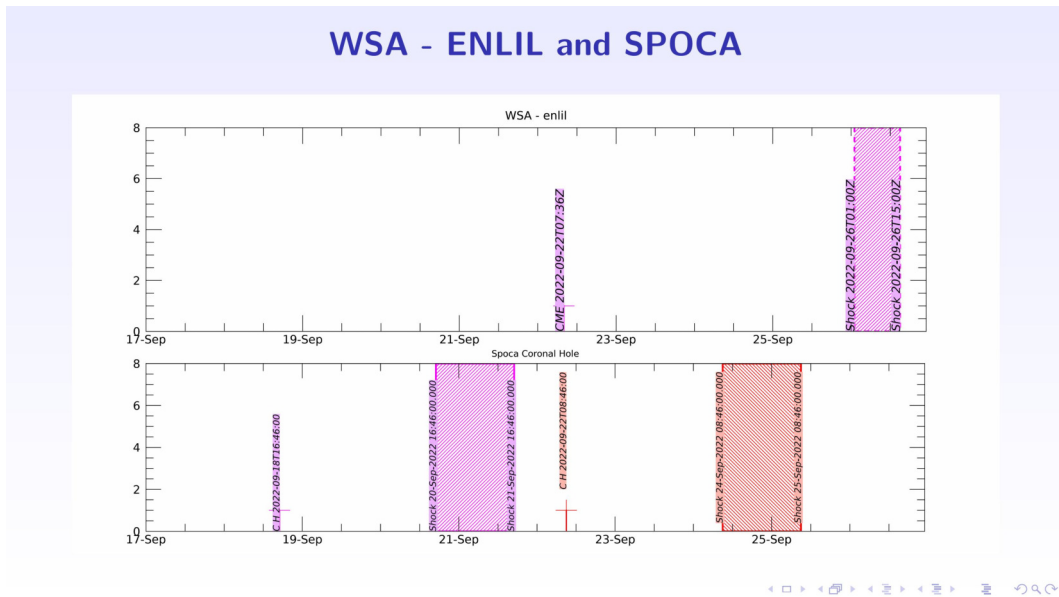


Figura: The solid line in black shows the products of the sum of areas for each detection interval performed by SPOCA between September 17 and 24, 2022.

Figura: Above the 193 Å image of the Sun are highlighted coronal holes observed by SPOCA around 16:46 UT on September 18, 2022 (red dot line).

Figura: Above the 193 Å image of the Sun are highlighted coronal holes observed by SPOCA around 08:46 UT on September 22, 2022 (blue dot line).

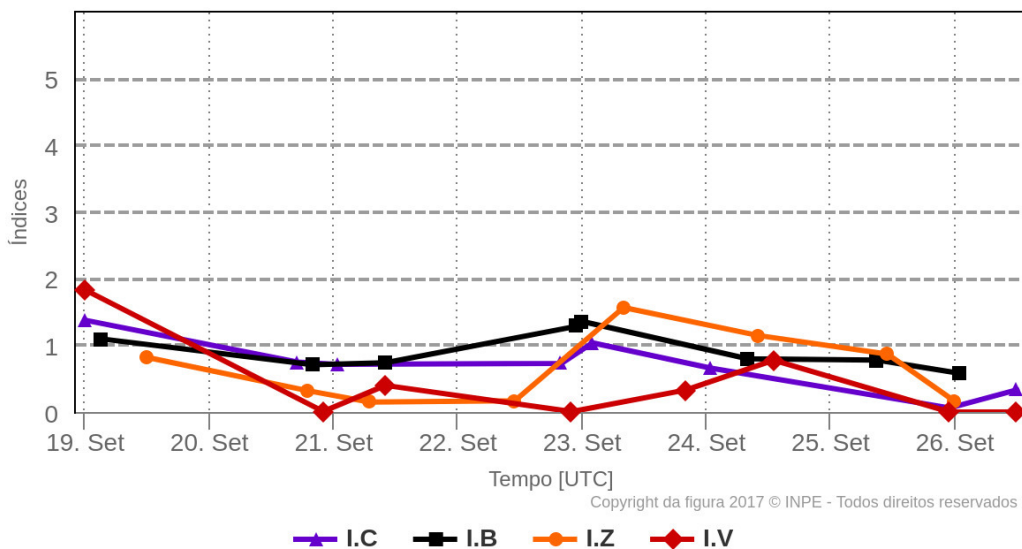


3 Interplanetary Medium

3.1 Responsible: Paulo Jauer

Resumo dos índices do meio interplanetário

Máximos diários - mais recentes entre 19 Set, 2022 e 26 Set, 2022



- The interplanetary medium region in the last week showed a low/moderate level of plasma perturbations due to the possible interaction of CME and HSS-like structures identified by the DISCOVER satellite in the interplanetary medium.
- The modulus of the interplanetary magnetic field component peaked at 10 nT on 23/Sep at 00:30 during the analyzed period.
- The BxBy components showed variations in the analyzed period, both remaining oscillating within the [+15, -15] nT interval, with the presence of sector switching on September 22, 23 and 24 at 09:30, 09:30 and 04:30 UT respectively.

- The component of the bz field presented a minimum value on Sep/23 07:30 UT of -6.6nT. On average, the component oscillated in the range of [+6, -6] nT.
- The solar wind density peaked at $16.4 p/cm^3$ on 23/Sep 02:30, however the density remained below $10 p/cm^3$ in the rest of the period.
- The solar wind speed remained mostly above 400 km/s during the analyzed period, changing its direction on September 25 at 00:30 UT.
- The magnetopause position was oscillating with a minimum value recorded on September 19 at 00:30 UT of 8.7 Re. The magnetopause showed a maximum expansion on 25/Sep at 16:30 of 12.8 Re.

4 Radiation Belts

4.1 Responsible: Ligia Alves da Silva

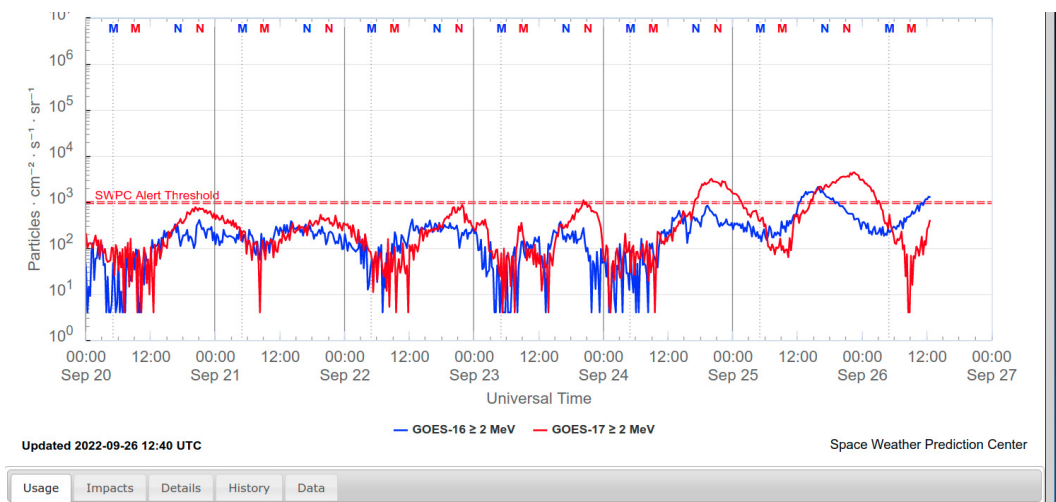


Figura 1: High-energy electron flux (> 2 MeV) obtained from GOES-16 and GOES-17 satellite. Source: <https://www.swpc.noaa.gov/products/goes-electron-flux>

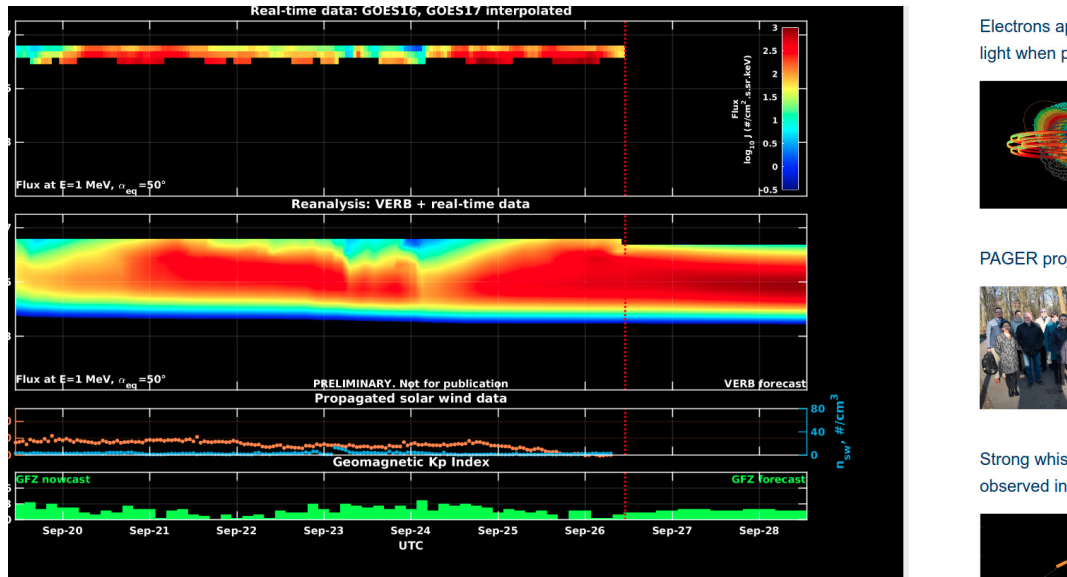


Figura 2: high-energy electron flux data (real-time and interpolated) obtained from GOES-16 and GOES-17 satellites. Reanalysis's data from VERB code and interpolated electron flux. Solar wind velocity and proton density data from ACE satellite. Source: <https://rbm.epss.ucla.edu/realtime-forecast/>

High-energy electron flux (> 2 MeV) in the outer boundary of the outer radiation belt obtained from geostationary satellite data GOES-16 and GOES-17 (Figure 1) shows significant variability during the analyzed period. Initially, the electron flux is considerably low, confined below 10^2 particles/(cm^2ssr) in the first 15 hours on September 20th. After that, an electron flux increase is observed, approaching the minimum threshold of 10^3 particles/(cm^2ssr), still on September 20th. The electron flux at the outer boundary of the outer belt was confined on average between 10^2 and 10^3 particles/(cm^2ssr) until September 24th. Significant decreases are observed on the 22nd, 23rd, and 24th of September, as well as increases that exceed the threshold of 10^3 particles/(cm^2ssr) on the 25th and 26th of September.

The GOES-16 and GOES-17 satellite data are interpolated and assimilated into the VERB code (Figure 2), which reconstructs this electron flux considering the Ultra Low Frequency (ULF) waves' radial diffusion. The simulation (VERB code) shows that the dropouts observed on the 23rd and 24th of September reached inner L-shells and the electron flux increases repopulated the outer belt in all L-shells. These electron flux variabilities coincide with the arrival of solar wind structures and ULF wave activities.

5 ULF waves

5.1 Responsible: Graziela B. D. Silva

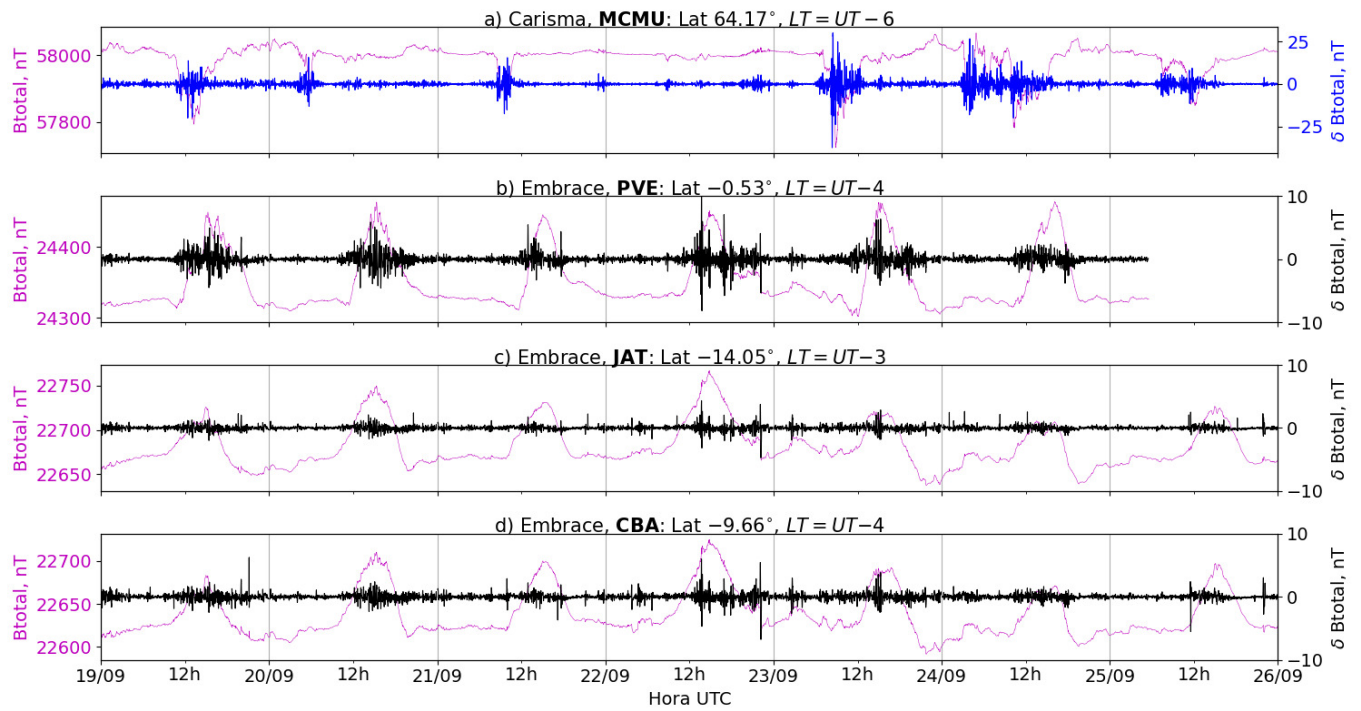


Figura 3: a) Timeseries of the geomagnetic field total component measured at MCMU station (Fort McMurray) of the CARISMA magnetometer network in magenta, along with the associated perturbation in the Pc5 band shown in blue. b-d) timeseries of the geomagnetic field total component measured at stations PVE (Porto Velho), JAT (Jataí), and CBA (Cuiabá) of the EMBRACE network in magenta, along with the Pc5 perturbation in blue.

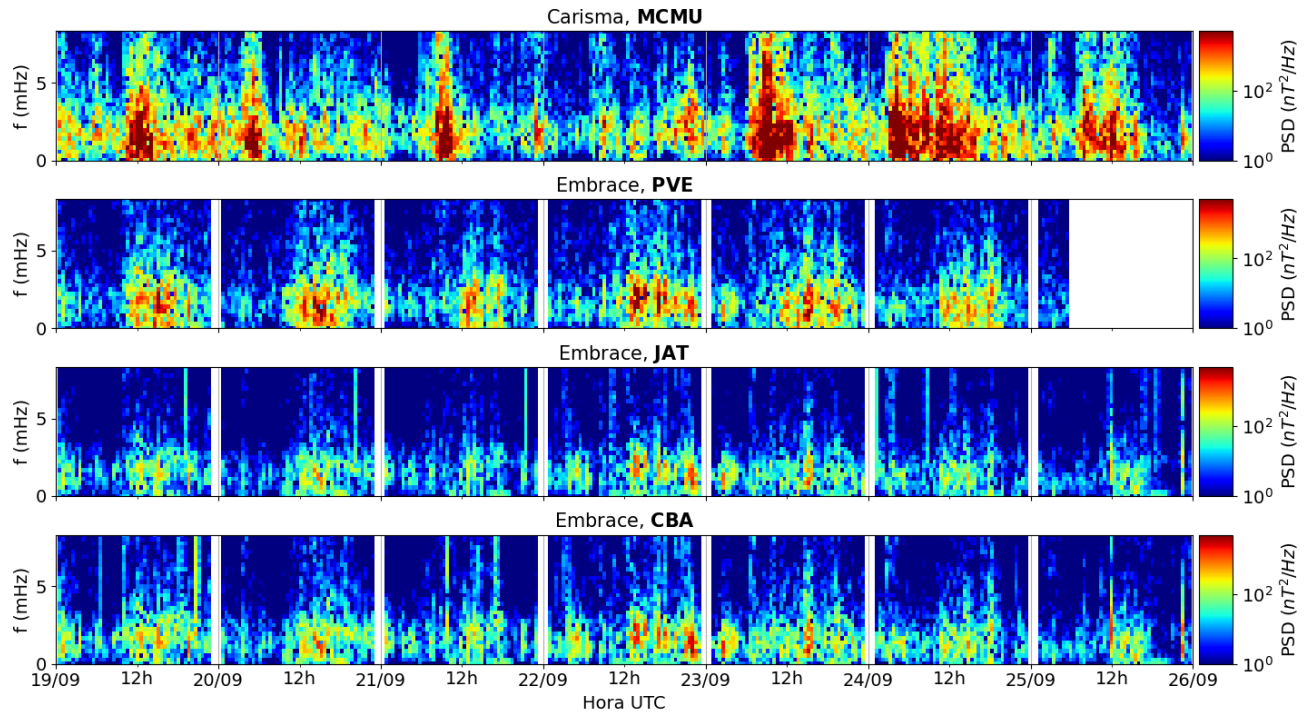


Figura 4: a-d) Time evolution of the power spectral density obtained from the filtered timeseries of the geomagnetic field total component (δB_{total}) for a) the high latitude station (MCMU-CARISMA), and b-d) for the low latitude stations of EMBRACE (PVE, JAT, CBA).

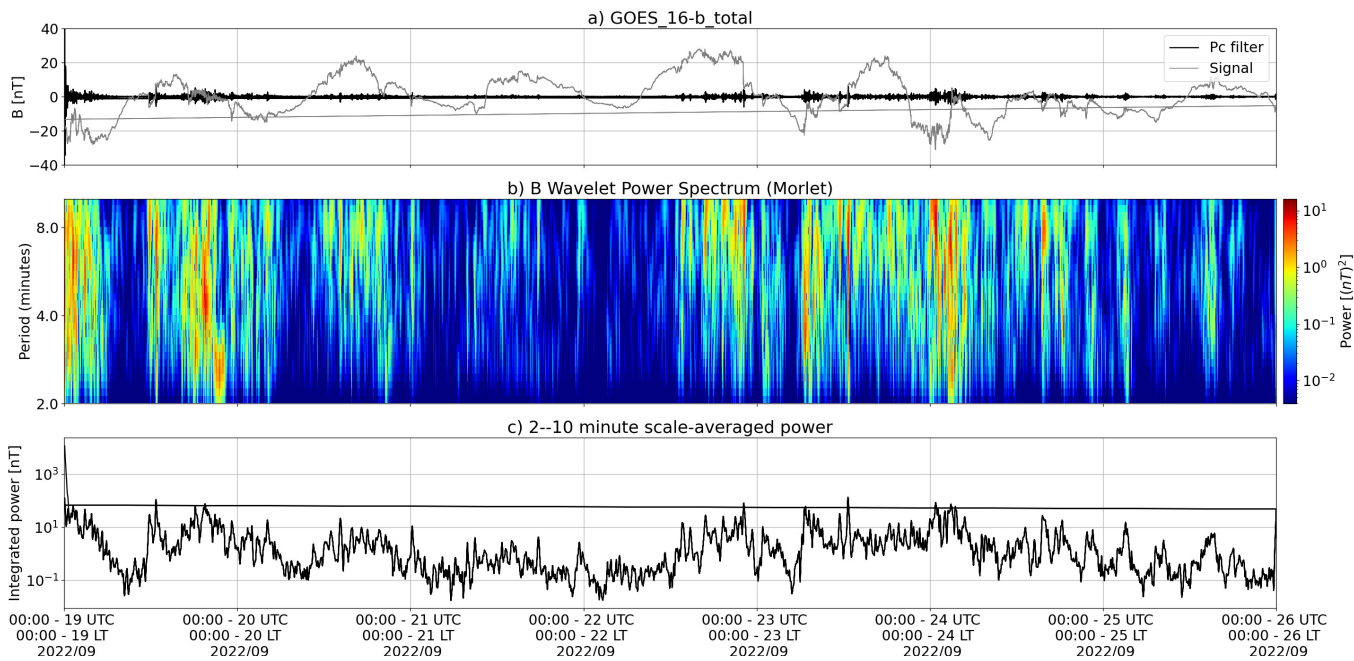


Figura 5: a) Timeseries of the geomagnetic field total component measured by GOES 16, together with the Pc5 fluctuation in black. b) Wavelet power spectrum of the filtered timeseries. c) Average ULF power in the period range from 2 to 10 minutes.

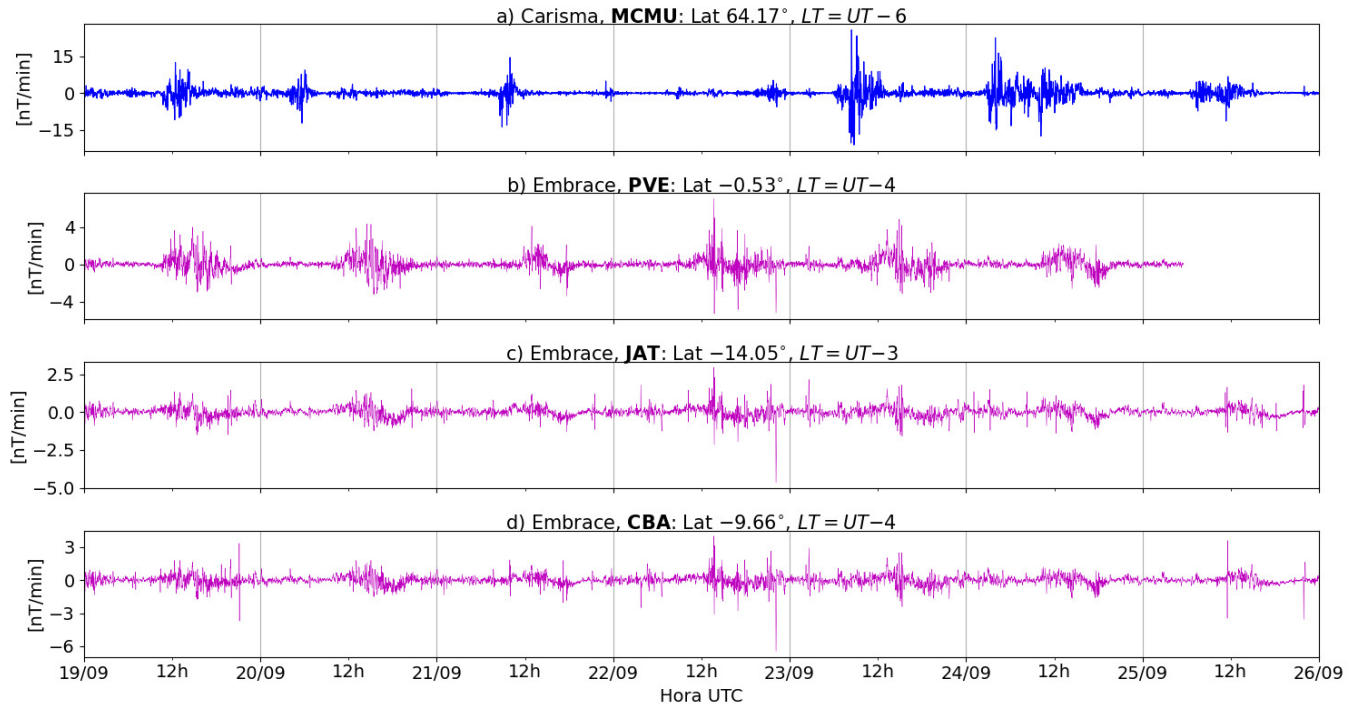


Figura 6: a-d) The rate of change of the geomagnetic field total component ($\delta B/\delta t$) obtained for a) the high latitude station (MCMU-CARISMA), and b-d) for the low latitude stations of EMBRACE (PVE, JAT, CBA).

- The GOES 16 satellite in geosynchronous orbit ($L \sim 6.6$) registered significant activity of Pc5 ULF waves on September 19 through Sep. 20, and from Sep. 23 onwards.
- As observed on the ground, the MCMU station of the Carisma network (high latitude, $L=5.35$) registered ULF wave activity throughout the week, especially from Sep. 23. The amplitude levels of the field fluctuations was in the interval $[-25, +25]$ nT.
- The low latitude stations of Embrace registered moderate to intense levels of ULF wave activity ($\delta B < 10$ nT), showing strong influence of the Equatorial electrojet on the wave activity observed at PVE station.
- The peaked and prolonged $\delta B/\delta t$ signals simultaneously observed at the low latitudes over Brazil did not surpass the threshold of 6 nT/min at CBA and JAT stations, but a recurrent prolonged $\delta B/\delta t$ activity associated with ULF waves occurrence was observed in PVE. The corresponding amplitudes were within $\sim [-5, +5]$ nT/min.

6 Geomagnetic activity

6.1 Responsible: Lívia Alves

In the week of September 20-26, the following events related to geomagnetic activity stand out:

- The data from the Embrace magnetometer network registered instabilities in Sep. 23-25.
- On Sep. 24, the magnetometers of the Embrace network recorded a significant drop in the H component.
- The geomagnetic field was active, the AE index was at 500 nT for several hours on Sep. 24. The Dst index reached -32 nT. The highest Kp of the week was 4-.
- The geomagnetic field measured at the GOES orbit shows instabilities on Sep. 24.

Briefing semana de 20/09 à 26/09 de 2022

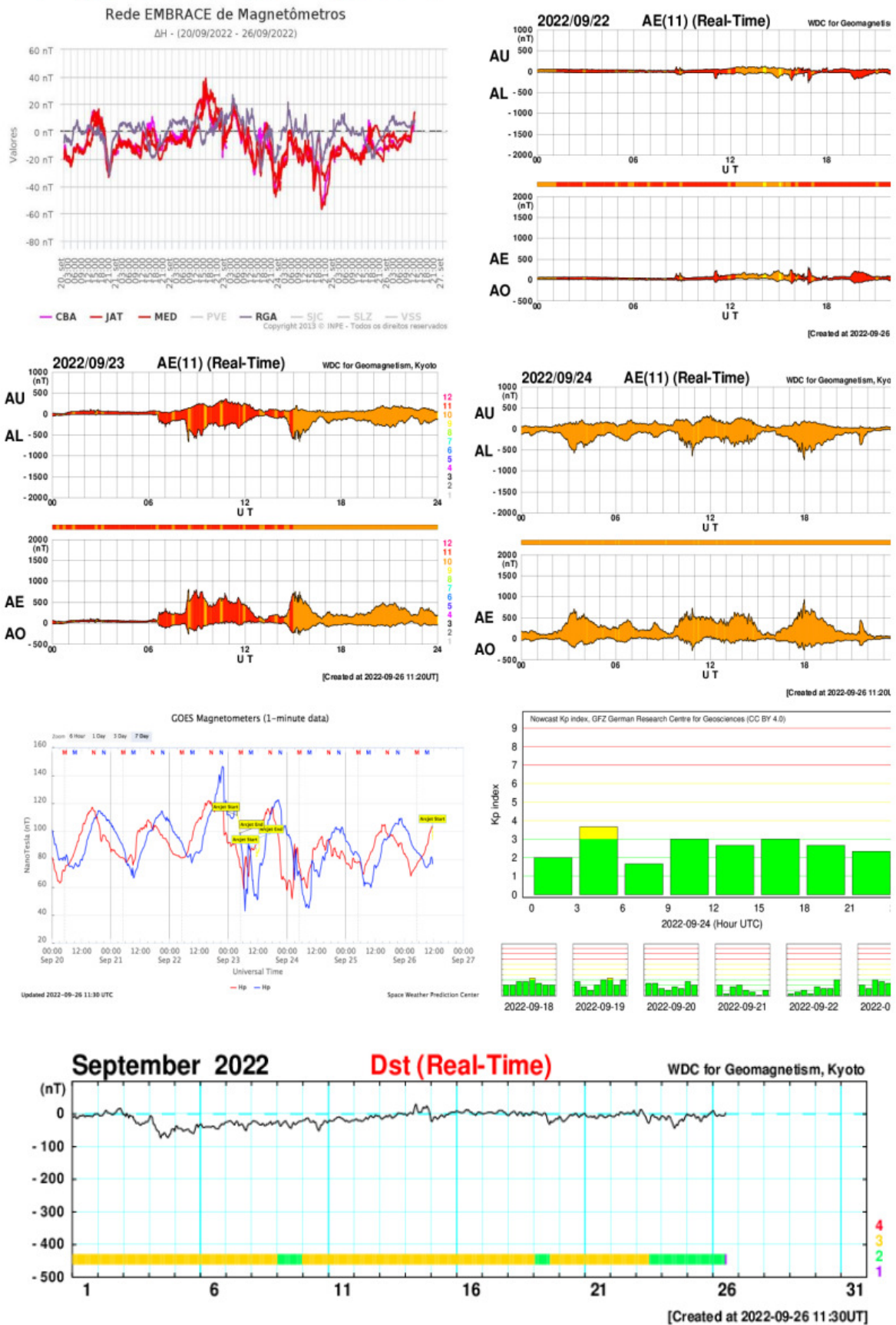
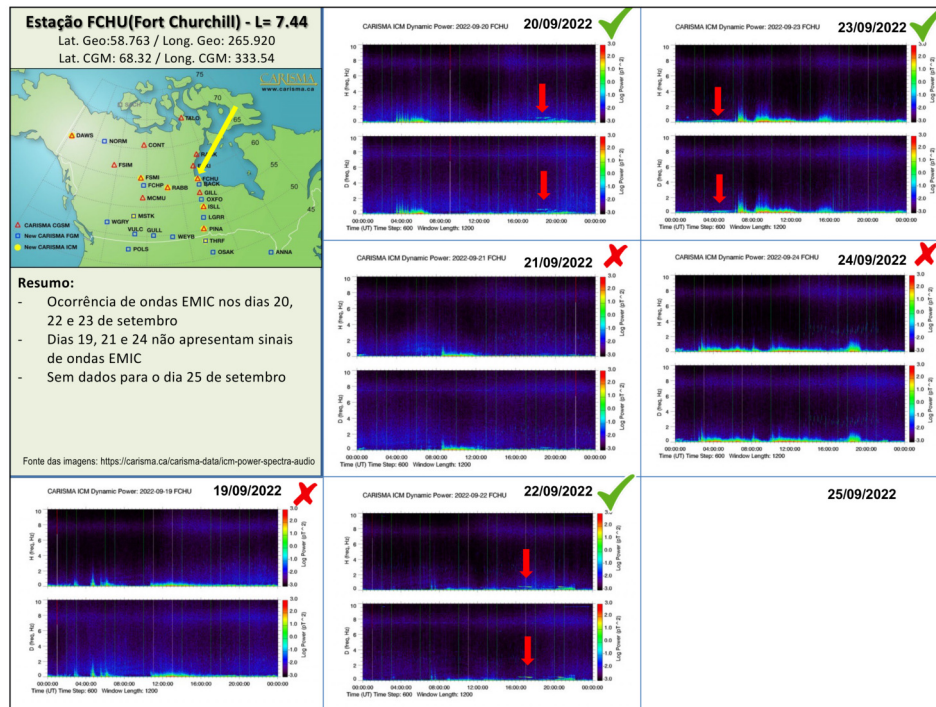


Figura 7: The figures from top to bottom show the weekly evolution of the H magnetic field component measured by the Embrace network, of the auroral AE index, of the geomagnetic field measured by the GOES satellites at $L \sim 6.6$ on the left, along with the Kp index on the right hand side. The bottom most figure contains the Dst index time series.

7 Ondas EMIC

7.1 Responsável: Claudia Medeiros



8 Ionosphere

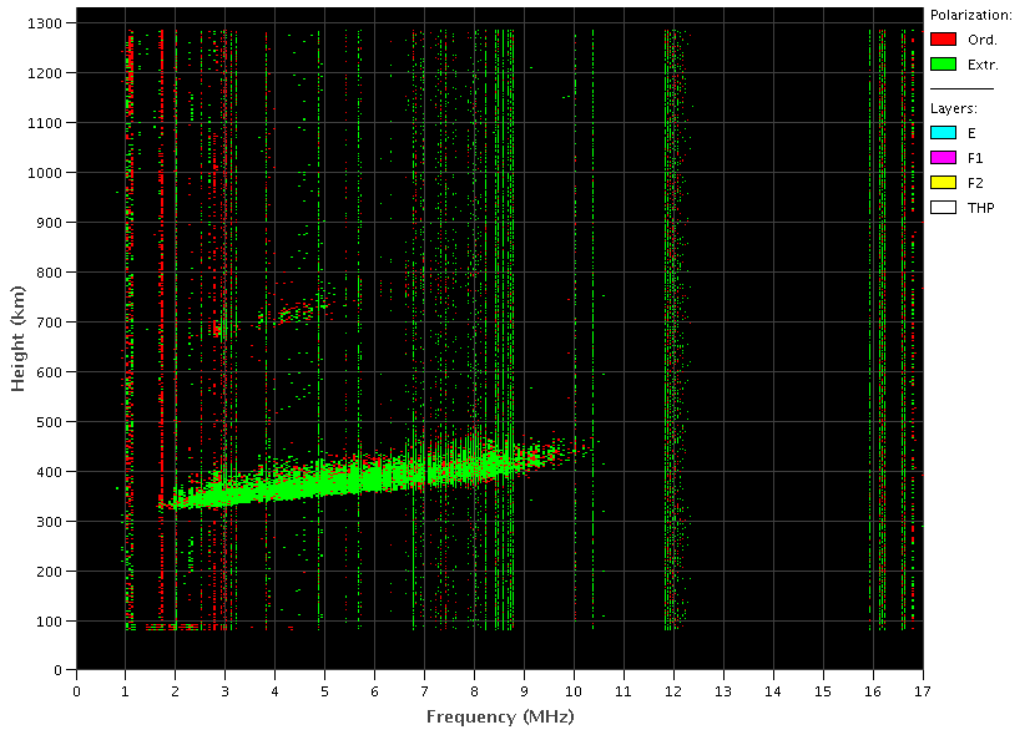
8.1 Responsible: Laysa Resende

Boa Vista:

- The spread occurred all days during this week.
- The Es layers reached scale 3 during the week.

EMBRACE – Digital Ionosonde

Boa Vista – 09/19/2022 00:40:00 UT



Cachoeira Paulista:

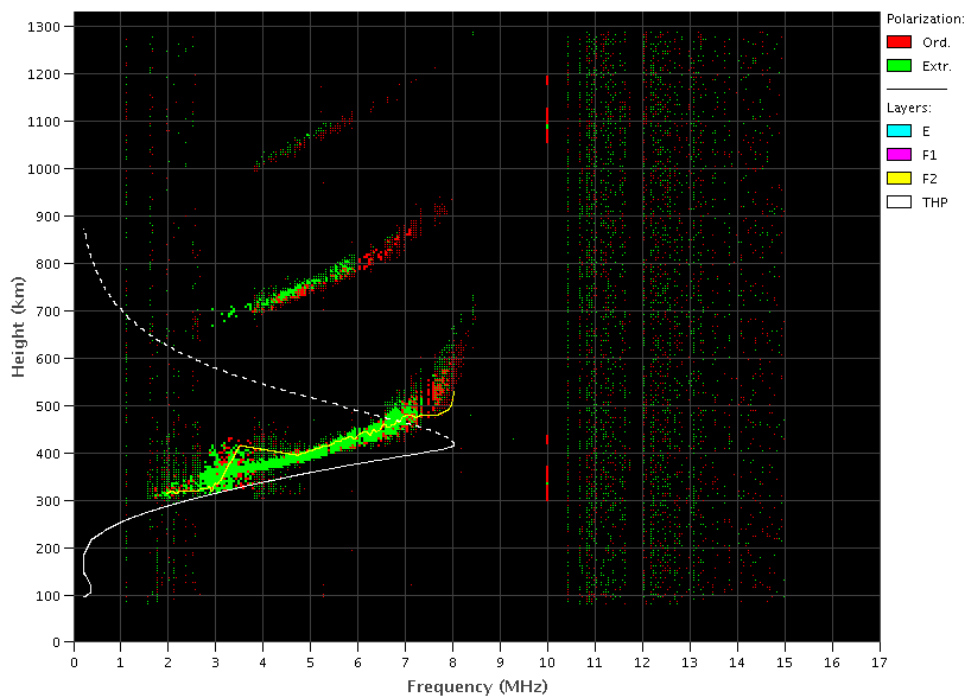
- No data.

São Luís:

- There were a spread during this week.
- The Es layers reached scale 2 during this week.

EMBRACE – Digital Ionosonde

São Luís – 09/19/2022 22:50:00 UT



9 Scintillation

9.1 Responsible: Siomel Savio Odriozola

In this report on the S4 scintillation index, data from SLMA in São Luiz/MA, STNT in Natal/RN, STCB in Cuiabá/MT and SJCE in São José dos Campos/SP are presented. The S4 index tracks the presence of irregularities in the ionosphere having a spatial scale ~ 360 m. From 19 to 21, scintillation activity was absent in STNT, STCB, and was mild in SLMA. From this date onwards S4 values greater than 0.4 were recorded for the rest of the week (Figure 1). The only station that did not show scintillation measurements above 0.2 was SJCE. The most severe events occurred between 25-26/09 for SLMA and STNT (Figure 2.) and between 22-23/09 for STCB.

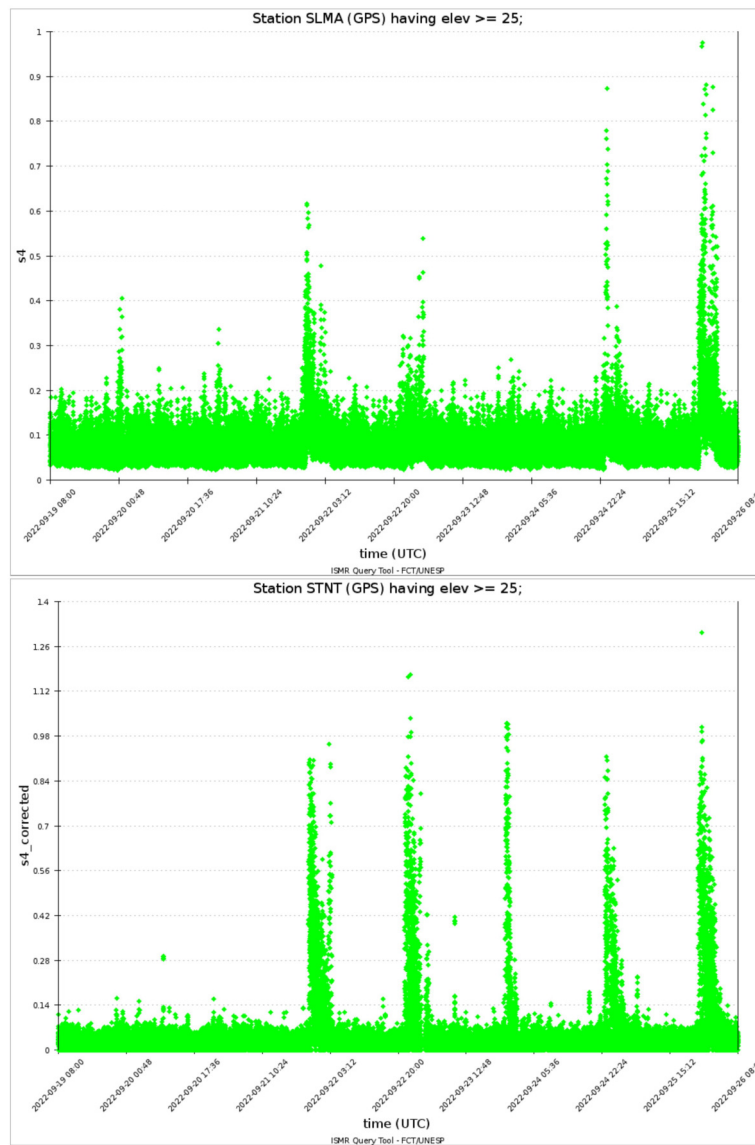
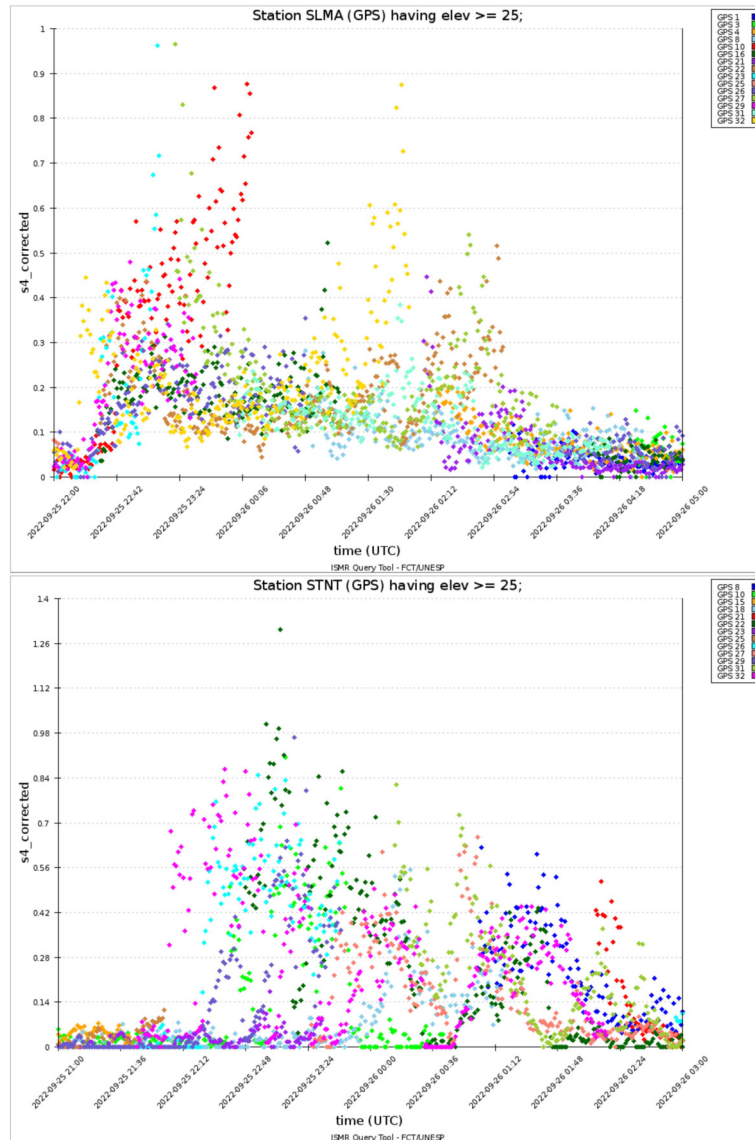


Figure 1: S4 index values for the GPS constellation measured at SLMA (upper panel) and STNT (lower panel) during the week 09/19 – 09/26.



S4 index values for the GPS constellation measured at the SLMA station between 22UT of the 25th to 05UT of the following day (upper panel) and STNT between 21UT of the 25th to 03UT of the following day (lower panel).

10 ROTI

10.1 Responsible: Carolina de Sousa do Carmo

In the week 2228 (September 18 to 24, 2022) there were ionospheric irregularities (plasma bubble), on all analyzed days, with the exception of the September 20, as shown in Table 1. In addition, Figure 1 shows an example of the plasma bubble occurrence on September 22, 2022, using keograms at -5° and -15° latitude.

Sunday	2022/09/18	00-03:30; 23:00-24:00
Monday	2022/09/19	00:00-04:00
Tuesday	2022/09/20	-
Wednesday	2022/09/21	22:00-24:00
Thursday	2022/09/22	00:00-06:00; 22:00-24:00
Friday	2022/09/23	00:00-04:30; 22:00-24:00
Saturday	2022/09/24	00:00-02:30; 23:00-24:00

Tabela 1: 24, 2022).

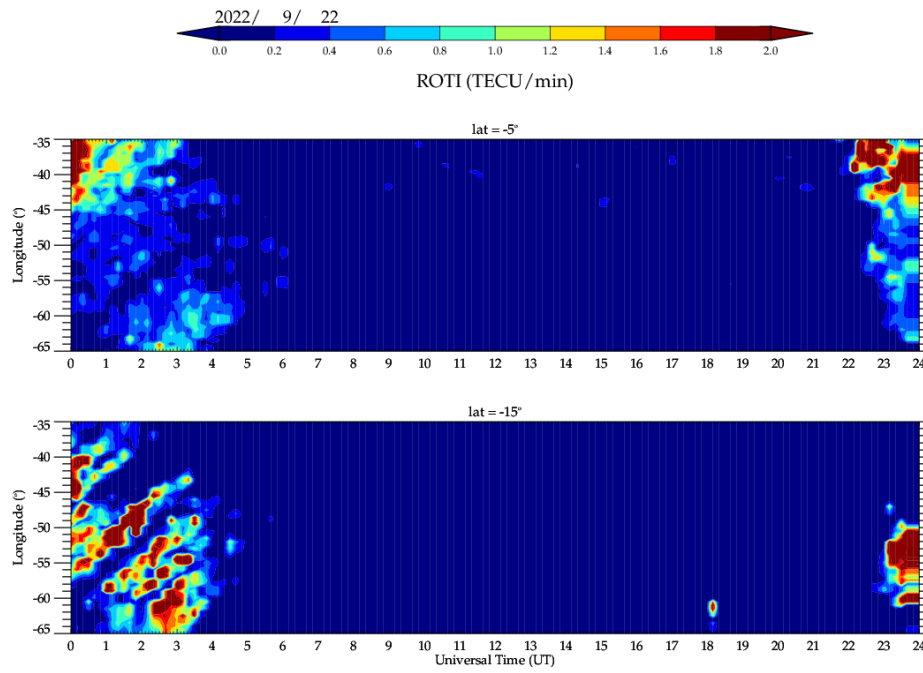


Figura 8: Keogram of September 22, 2022, for latitudes of -5° and -15°